Received 5 June 2023, accepted 18 September 2023, date of publication 2 October 2023, date of current version 20 October 2023.

Digital Object Identifier 10.1109/ACCESS.2023.3321339

RESEARCH ARTICLE

Application of Electrical Breakdown in Liquid Process on Inulin Structural Transformations

KHANIT MATRA[1], WANATTAPONG ARYUWONG[1], WICHAYADA MEETANG[1], SUPARADA RUTHAIRAT[1], CHANCHAI DECHTHUMMARONG[2], WUTTHICHOK SANGWANG[3], AND VIJITRA LUANG-IN[4]

[1]Department of Electrical Engineering, Faculty of Engineering, Srinakharinwirot University, Nakhon Nayok 26120, Thailand
[2]Department of Electrical Engineering, Faculty of Engineering, Rajamangala University of Technology Lanna, Chiang Mai 50300, Thailand
[3]Thailand Institute of Nuclear Technology (Public Organization), Ongkharak, Nakhon Nayok 26120, Thailand
[4]Natural Antioxidant Innovation Research Unit, Department of Biotechnology, Faculty of Technology, Mahasarakham University, Maha Sarakham 44150, Thailand

Corresponding authors: Khanit Matra (khanit@g.swu.ac.th) and Vijitra Luang-In (vijitra.l@msu.ac.th)

ABSTRACT This work proposes a novel technique for biological compound transformation by a circulating electrical breakdown in the liquid (EBL) process. The EBL reactor has been designed with a cylindrical, hourglass-shaped structure that facilitates plasma generation within a 1 mm gap between two pin electrodes at the neck of the reactor. During the EBL process, the inulin solution was flown upward and brought into direct contact with the plasma before recirculating back to the bottom of the reactor for subsequent retreatment. Consequently, it enabled a continuous and thorough inulin treatment. At this time, the influence of the supplied voltage (3.20, 3.76, and 4.32 kV_{peak} at 50 Hz positive half-wave) for the EBL process generation on the inulin structural transformation was investigated. The most optimal condition in the EBL process was operated at 4.32 kV_{peak} supplied voltage within the optimal inulin treatment duration of 20 min. Regarding the experimental results, it could be confirmed that the EBL process has the potential to depolymerize the inulin structure. One gram of inulin was dissolved in 100 mL of deionized water and treated under the EBL process for 20 min. Inulin structures were deformed from a 20-100 μm micro spherical shapes into small flakes. Moreover, the DPPH free radical scavenging analysis showed that the antioxidant activity and the prebiotic activity of treated inulin have been improved by 311%, and 35%, respectively.

INDEX TERMS Inulin, polysaccharide, depolymerization, antioxidant, plasma—liquid interactions, solution plasma processing.

I. INTRODUCTION

An inevitable negative by-product of the rapidly evolving world is the massive daily production of waste, which has a huge impact on ecosystems and humans. Therefore, how to reduce and recycle wasted products is essentially the focus. Each year, more than a thousand tons of agricultural residues have been abandoned owing to imperfect preference, including problems in harvesting and processing. However, the imperfection of those agricultural residues has not affected their beneficial nutrients. Therefore, many researchers have been looking for new ways to turn these products into value-added products, such as cosmetic ingredients, supplementary food, prebiotics, medicines, and others [1], [2], [3], [4].

In classical electrical engineering, electrical breakdown in liquid (EBL) seems to be a major problem if it happens in liquid-insulating materials [5], [6]. However, this electrical breakdown in liquid, also known as in-liquid plasma or solution plasma processing (SPP), has recently received much attention in the field of applied high voltage applications owing to advanced oxidation processes (AOP) of active free reactive radicals, such as reactive oxygen species (ROSs), reactive nitrogen species (RNSs), and reactive oxygen-nitrogen species (RONSs) productions; in the chemical reactions generated during the in-liquid breakdown process [7], [8], [9], [10], [11]. These chemical reactions can help reduce the number of organic contaminants in the liquid.

The associate editor coordinating the review of this manuscript and approving it for publication was Mohd Tariq.

In addition, the EBL process also enhances the biological structure modification of organic matter (biotransformation). The shorter size or reduced molecular weights of organic matter, such as the polysaccharide structure, are beneficial for bioactive functions and intrinsic viscosity [12], [13], [14]. Moreover, many useful phenomena also happen during the ELB process, such as kinetic reactions, electric fields, electromagnetic waves, photons, shockwaves, and ultraviolet rays [7], [8], [9]. Therefore, the EBL process can also be beneficially applied to waste disposal, food, pharmaceutical, cosmetic, medical, agricultural, and chemical industries [8], [9], [14], [15], [16], [17], [18], [19], [20], [21].

At this time, the influence of electrical breakdown in the liquid process on structural transformations of biological compounds from agro-industrial waste materials has been investigated. In this work, inulin, one of the most beneficial functional foods in the group of natural polysaccharides numerously used in both food and medicine, has been chosen to be investigated. Inulin, a dietary fiber found naturally in plants like chicory, garlic, Jerusalem artichoke, onion, leeks, and asparagus, is classified as a fructan-type non-digestible carbohydrate. It serves as a vital functional ingredient for improving digestive health. In the culinary realm, inulin is used in a variety of food products. Genially, inulin resists digestion by human pancreatic enzymes but can be metabolized by gut microorganisms. This dual role as a non-digestible fiber and a prebiotic (substances found in food that promote the development or stimulation of advantageous microorganisms) makes it a valuable contributor to gut health, benefiting both the small and large intestines [4], [22], [23], [24]. Important functionalities of inulin, such as solubility, thermo-stability, sweetness, and prebiotic action, are related to the existence of branches and the degree of polymerization [4], [22], [25]. Therefore, it is expected that the EBL process would enable value addition and enhance the bioactive functions of inulin, which is extracted from artichoke roots, an emerging agricultural waste. In this work, the EBL reactor was initially designed for practical use for inulin biotransformation at laboratory scale with low cost prior to extrapolation to a larger scale. The effect of the EBL process on the inulin structure and antioxidant activity was investigated by a scanning electron microscope (SEM), and a 2,2-diphenyl-1-picrylhydrazyl (DPPH) scavenging assay, respectively. The electrical characteristics of the in-liquid electrical breakdown process was also monitored and analyzed.

II. EXPERIMENTAL SETUP AND METHODS

A. PLASMA MODEL AND EXPERIMENTAL SETUP

Fig. 1 elucidates the illustrative drawing of the electrical breakdown in the liquid (EBL) process and the experimental setup. The plasma reactor for the EBL process is cylindrical and hourglass-shaped with four Ø5 mm ports for in/outlet of water, and air, made from Pyrex glass. The thickness and inner diameter of the reactor at the shortest and common parts are 2, 5, and 10 mm, respectively. At the shortest gap of the reactor, two Ø0.1 mm tip tungsten rods (2% lanthanated tig tungsten electrode) have been inserted into the sidewall oppositely as high voltage electrodes for the EBL process. The gap between these two electrodes is 1 mm. The EBL process is a circulating system, in which a target solution is circulated between the rector and reservoir beaker via Peristaltic Pump DP-385 into and out of the plasma reactor at a pumping rate of 42 ml s^{-1}.

The target solution was flown from the reservoir beaker into the reactor, and back to the reservoir beaker again as a circulated treatment system. Air bubbles from the air compressor (HAILEA ACO-318) have been supplied to the space between electrodes in the reactor from the bottom air inlet at a flow rate of 1 LPM. To start the EBL process, one side of the tungsten electrode has been connected to the high voltage supplied from a positive half-wave voltage doubler (HWVD) circuit from an 800 W microwave transformer, while the other electrode is connected to a 17.5-ohm monitor resistor in series, and then grounded. The maximum output voltage used at this time is 4.32 kV_{peak} at the input voltage of 150V_{rms} from 50 Hz variable ac power supplies [26]. Regarding the EBL process, heat could be accumulated in the solution; therefore, the solution has been kept between 25 - 29^{o} C by using a 5^{o}C cooling system.

To monitor the electrical properties of the discharge voltage (V_D) and current (I_D), an oscilloscope (GW Instek GDS-1104B, 100 MHz, 1 GSa/s) has been used. A high-voltage probe (Pintek HVP-28HF, 75 MHz bandwidth) has been connected across the plasma model, and a general-purpose passive probe (GW Instek, 100 MHz bandwidth) was connected across the monitored resistor. To study optical emission spectroscopy (OES) during plasma formation, a small charge-coupled device (CCD) spectrometer (Newport 71SI00087) has been employed. The optical fiber detector tip was perpendicularly 1 cm away from the electrode plane.

B. EBL TREATMENT PROCESS

The target solution (1 mg of inulin powder (purchased from Krungthepchemi Co., Ltd.) dissolved in 100 mL of deionized water (DI water) were treated by the EBL process at three different input voltages of 110, 130, and 150 V_{rms} for 20 min (a maximum continuous operating time of power supply), respectively. It should be noted that this work mainly focused on determining the optimal input voltage at a 20-min treatment time. The processing time at 20 min had been chosen and thought to suffice to trigger the depolymerization of inulin (polysaccharide) because it had recently been proved that the EBL process is able to decrease the molecular weight of chitosan (another polysaccharide) from an initial 197 kDa to 9-40 kDa after 20 min of plasma treatment utilizing a DC glow discharge initiated between a graphite anode and the surface of a chitosan solution acting as cathode [27].

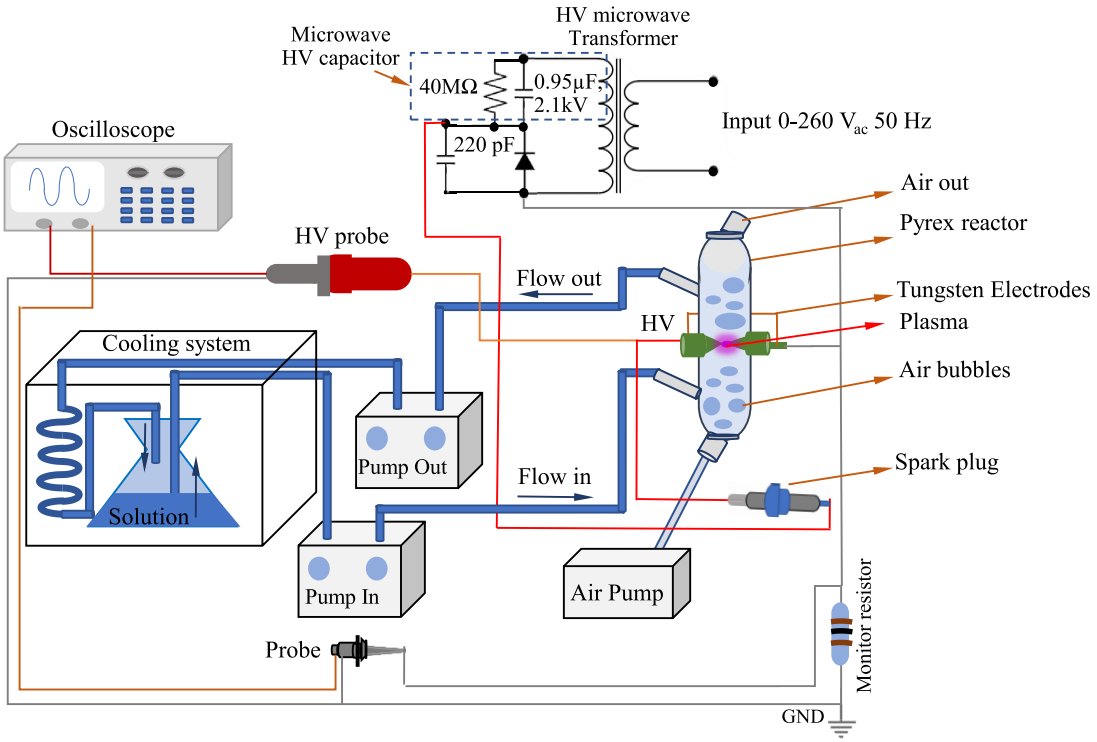

FIGURE 1. The illustrative drawing of EBL process and the experimental setup.

C. CHARACTERIZATION OF PLASMA-TREATED INULIN

1) PREPARATION OF PLASMA-TREATED INULIN FOR ANALYSIS

Control samples (no plasma treated) and plasma-treated inulin were freeze-dried and then used for structural analysis. Freeze-dried samples were redissolved in deionized water to make a 20 mg mL^{-1} stock solution for the antioxidant assay. As for prebiotic property assessment, inulin solutions were used directly after plasma treatment.

2) PHYSICAL AND CHEMICAL ANALYSIS OF INULIN SOLUTION

The physical-chemical properties of inulin solution, including pH, temperature, and electrical conductivity (EC), were investigated. A pH meter (model SevenEasyTMpH, Mettler Toledo) and a conductivity meter (model HI4321, Hanna) were used to monitor the pH levels and EC, respectively. The solution temperature was monitored by a mercury thermometer immersed in a treating solution. The Quantofix peroxide 25 test strips verified that H_2O_2 was produced in the PAW.

3) STRUCTURAL ANALYSIS

The morphology of inulin samples was analyzed by scanning electron microscopy (model Hitachi S-3500N) at Central Laboratory Center at Mahasarakham University, Thailand.

4) ANTIOXIDANT ACTIVITY ANALYSIS

2,2-Diphenyl-1-picrylhydrazyl (DPPH) scavenging activity assay was used to assess the antioxidant activity of inulin. The procedure was previously described in [28]. Trolox was used as a standard and expressed as μg Trolox Equivalent TE mL^{-1}.

5) PREBIOTIC ACTIVITY

Plasma-treated inulin or untreated inulin (1 g per 100 mL) solutions (5 mL) or sterile deionized water (negative control) (5 mL) were sterilized using 0.22 μm membrane filter and added to 5 mL MRS broth (from De Man, Rogosa, and Sharpe) of 1% v/v bacterial culture inoculum of *Lactococcus lactis* subsp. *lactis* TBRC 375. Over the course of 72 h, 1 mL of culture was taken for OD_{600nm} measurement at 8, 24, 32, 48, 56, and 72 h. Growth curves were constructed.

D. STATISTICAL ANALYSIS

All experimental conditions and measurements have been rigorously validated through triplicate testing to derive the mean result value. Statistical significance was tested at $p < 0.05$ using Duncan's Multiple Range Test.

III. RESULTS AND DISCUSSION

A. ELECTRICAL MODEL AND VISUAL CHARACTERISTICS OF THE EBL PROCESS

In order to generate the discharge under the liquid phase with a small high voltage and a large frequency, the electrode geometry is necessary to be sharp in order to cause a highly non-uniform electric field, resulting in electrical stress at the intermediate voltage. Therefore, plasma reactor for the EBL process in this work is composed of a couple of pin electrodes separated by a small space as shown in Fig. 1. The maximum electric field strength (E_{Max}) at the anode tip was expressed by equation (2), modified from [29] and [30]

$$E_{Max} = \frac{V_{anode}}{\ln\left(\frac{1+\eta_0}{1-\eta_0}\right)}\left(\frac{a}{a^2-(d/2)^2}\right), \quad \mathrm{kV\ cm^{-1}} \qquad (1)$$

where d is the distance between two electrode tips and R is the radius of the cultivarue of the electrode tip. $a = [(d/2)(d/2 + R)]^{1/2}$ and $\eta_0 = [(d/2)/(d/2 + R)]^{1/2}$. V_{anode} is the potential at the anode tip while $V_{cathode}$ is zero (grounded). Air discharge is typically initiated when the electric field strength surpasses a critical threshold of 31 kV cm^{-1}. In the specific experimental setup, a peak voltage of 4.32 kV resulted in the E_{Max} of approximately 69.31 kV cm^{-1}, which is sufficient to induce air discharge in the atmospheric environment. However, the discharge phenomena in liquid media containing air bubbles are notably more complex than those in atmospheric conditions. This complexity arises due to the interaction between the electric field, the bubble dynamics, and the liquid environment [31], [32], [33], [34], [35], [36].

When the EBL process has been started, an electrical breakdown (plasma) has been generated in the space between sharp electrodes. At the beginning of the process, plasma is difficult to generate due to the low liquid electrical conductivity (EC), which is around 0.01 mS cm^{-1}. In the initial stages, the input voltage is gradually raised to an intermediate point before reaching the setup input voltage. The breakdown occasionally arises when the air bubble reaches around the electrodes (in-bubble contacted discharge). However, the breakdown has often been generated gradually with treatment time increase due to the increasing EC of liquid regarding EBL process (data presented in section III-D. The discharge mechanism observed in this phase is similar to the discharge mechanism that occurs at the electrode-gas interphase in the atmospheric environment [31], [32], [33], [34], [35], [36]. Fig. 2 illustrates examples of the visual time evolution characteristics of the EBL process when the process has reached a stable state (less EC change). It should be noted that the visual characteristics investigated in this study have been recorded using a camera with a fixed frame rate of 177.2 frames per second and a fixed size of 1080 pixels. The time development of the picture has been used as a basis for analysis, with sample stills captured at 1, 3, 11, and 15 ms. However, it should be emphasized that a video camera with a greater frame rate is required to catch the delicate details of the process and achieve a complete grasp of the visual characteristics associated with discharge development. It could be observed that the corona streamer discharge has initiated a pre-breakdown in the liquid phase (in-liquid contacted discharge), owing to micro gas bubbles initiated from the joule heating, at both highly-stress electrode tips (Fig. 2a)) [31], [32], [33], [34], [35], [36], [37]. As time increased, a streamer has been developed and bridged across both tips to become a plasma column (Fig. 2b)). When the air bubbles have arrived near the plasma column (in-bubble contacted discharge), the breakdown has developed to a spark streamer discharge and greatly expanded, consistent with the air dynamic bubble deformation due to the internal and external non-uniform electric field distribution of bubbles [38], [39], [40] (Fig. 2c) and 2d)). Finally, at the time the air bubble has deformed and completely traveled past the electrode gap, the breakdown has been terminated, and then start the new cycle again [38], [39], [41]. It should be noted that distinctive voices from the explosion when a spark streamer discharge is taking place could be noticed during the EBL process, indicating the shock wave generation corresponding to the pulsed breakdown [37], [42].

B. ELECTRICAL CHARACTERISTICS OF THE EBL PROCESS

In Fig. 3, the comparison of the electrical characteristics of the electrical breakdown under water at various treatment times is illustrated. At the input voltage of 110 V_{rms}, 130 V_{rms}, and 150 V_{rms}, the peak voltage at no load conditions is around 3.20, 3.76, and 4.32 kV, respectively. It should be noted here that the electrical characteristics of discharge voltage and current of all input voltages perform in a similar trend but different magnitude; therefore, only electrical characteristics of 150 V_{rms} input voltage have been elaborated. The voltage waveforms are shown in 50 Hz positive half-wave. The on time of voltage is around 17.5 ms. It could be clearly seen that the magnitude of discharge voltage (V_D) across electrodes has decreased when increasing the treating time, as shown in Fig. 3a). The breakdown voltage (the maximum V_D before dropping) during the EBL process at 1, 10, and 20 min is around 3.36, 1.88, and 1.48 kV_{peak}, respectively. During the discharge, there is an increasing in discharge current (I_D) corresponding to the dropping of V_D, as shown in Fig. 3b). During the EBL process at 1, 10, and 20 min, the I_D peaks are in the ranges of 0.72-6.12, 0.60-3.48, and 0.36-3.24 A_{peak} with the pulse width around 0.5 μs, respectively. The characteristics of I_D are similar to a micro discharge in which the self-pulsing discharge pulse width are in the range of microseconds [43], [44], [45]. However, the frequency of these self-pulsing discharges is quite dynamic owing to the turbulently floating bubble, flowing solution, and EPL process.

Fig. 3c) depicts a zoom-in image of one loop of waveform characteristics at 1 min, which is in the red rectangle in Fig. 3a) and can be used to explain the V-I characteristics of

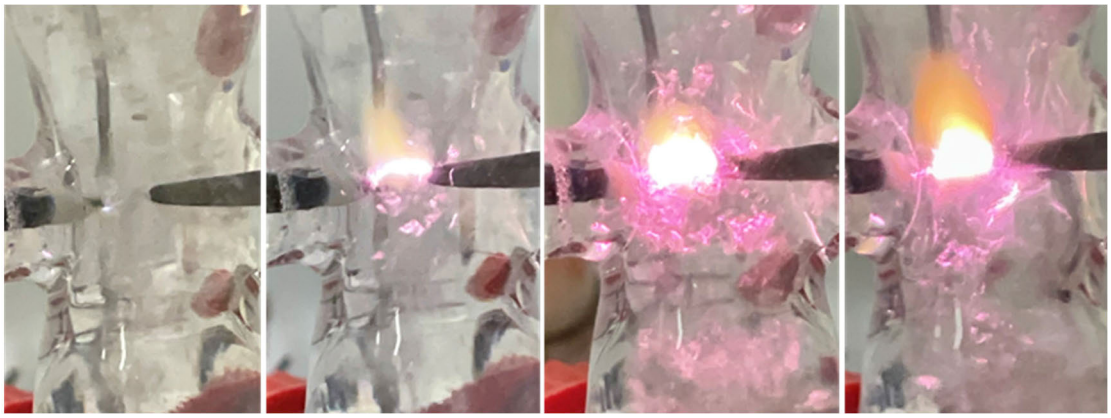

FIGURE 2. Time evolution example images of visual characteristics of EBL process.

this work. The discharge current in plasma is a consequence of electrical discharge. When there is no plasma, there should be no discharge current in the circuit, and the voltage across the plasma model should be close to the supply voltage with minimal voltage loss. However, if the supplied voltage is high enough, the liquid breakdown can occur causing the voltage across the plasma model to drop while the discharge current increases.

The high-voltage power supply unit used in this work provides a 50 Hz positive half-wave high voltage with a period of A_1-A_2 at no load. The on time of the supplied voltage is around 17.5 ms (A_1-F), and electrical discharges are generated during the on time of the supplied voltage in each cycle (main loop). The mechanism of one-cycle discharge of the main loop can be explained as follows: the voltage across the electrode during the EBL process starts at A_1, the same as in the no-load condition. It is important to note that the voltage across the electrodes during the EBL process slightly drops compared to that of the no-load condition due to the leakage current and joule heating in the conductive liquid. When the electrode voltage increases to B, the discharge is initiated, resulting in an abrupt drop in the electrode voltage together with an instantaneous increase in discharge current. At this point (B), there is a short transition around 20 ns from streamer discharge to spark discharge as depicted in Fig. 3d) [33], [46], [47], [48]. However, other sub sequential micro discharges can still be generated during the increase of the supplied voltage beyond the breakdown voltage (B-C) due to leftover free ions and electrons from previous discharges. These micro discharges terminate at phase C since the capacitor of the power supply unit has discharged all the stored voltage (charges) generated during micro discharge, resulting in no discharge in phase C-D. Nevertheless, during this period, the capacitor is still being charged from the transformer. The capacitor will discharge again when it gains enough voltage higher than the breakdown voltage at phase D. However, the micro discharges occur only during phase D-E before the capacitor has discharged all the stored voltage again. It is important to note that phase D-E has a marginally shorter duration than phase B-C. Since the capacitor was charged during the declining edge of the supplied voltage, there is a brief period of time after phase D-E during which it can be charged with a voltage greater than the breakdown voltage. Therefore, the main loop discharge terminates at phase E. The discharge will start again at the same principle at phase A_2, periodically.

During the EBL process, it could be clearly noticed that the temperature of the treating solution had increased very quickly. Regarding the preliminary experiment, it should be noted that the temperature of a static treating solution could be heated up from 25 to 60 °C within 30 s; therefore, the circulated cooling system has been applied in this work. This phenomenon could be evidence of joule heating loss in the treating solution, in which the EC has been increasing with time [49], [50], [51], [52].

During the EBL process, the advanced oxidation processes (AOP) of active free radicals in the treating solution have played an important role in an increase in the EC of the solution [7], [8], [9]. The increased EC has resulted in a reduction of solution resistance; therefore, the high temperature would accumulate in the treating solution during the EBL process as a result of an electro-thermal process due to a significant leakage current [52].

The active energy consumption per pulse during the EBL process could be derived from the integration over the duration of the V_D pulse (T_P) of V_D and I_D, as in

$$W_{per\ pulse} = \int_0^{T_p} V_D(t) I_D(t) dt, \quad \text{J pulse}^{-1} \tag{2}$$

The discharge energy levels at the treatment time at 1, 10, and 20 min were approximately 97.99, 83.89, and 38.44 mJ pulse^{-1}, respectively [53], [54]. The discharge energy tends to decrease as the treatment time increases due to the loss from joule heating and a leakage current in a high-EC solu-

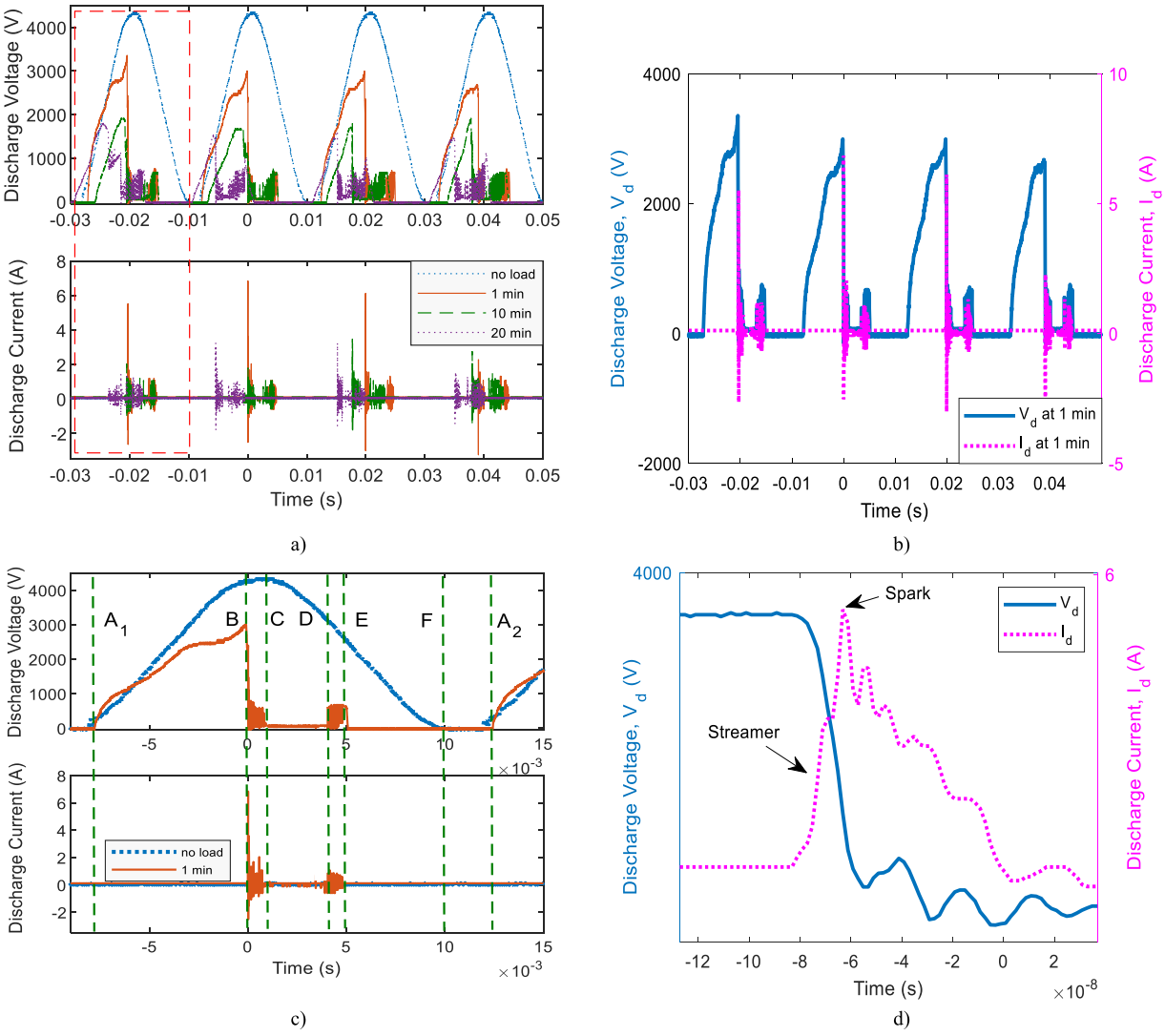

FIGURE 3. a) Time evolution of discharge voltage and current characteristics at varous treatment times, b) discharge wavefrom characteristics at 1 min, c) one loop of wavefrom characteristics at 1 min, and d) discharge wavefrom characteristics at the small time scale, during EBL process at the input voltage of 150 V_{rms}.

tion. A smaller equivalent impedance, compared to that of the air bubble, of treating solution resulting from the increasing of EC causes a huge energy loss into the solution and a reduction of energy efficacy [52], [55], [56]. Therefore, the discharge current tends to be suppressed quicker when the EC increases, as shown in Fig. 3a) [56].

C. OPTICAL EMISSION SPECTRUM CHARACTERISTICS OF THE EBL PROCESS

During the EBL process, the optical emission spectra (OES) have been investigated, as demonstrated in Fig. 4. Regarding the non-continuous discharge under water, the OES has varied with time due to the different discharge phenomena, streamers, and spark discharges. Therefore, the three most frequently observed OES during the EBL process have been comparably plotted. It should be noted that the legend in Fig. 4 represents the OESs observed at 3 different capturing times. It could be commonly observed in 3 cases that the atomic oxygen emission at 777.4 and 844 nm, as well as the highly reactive species of OH· at 309.6 nm, could be detected. The N_2 second positive system has been observed in the range from 310 nm to 400 nm. H_β and H_α lines could be seen at 486.13 and 656.28 nm, respectively [57], [58], [59], [60], [61], [62], [63], [64]. These radicals have played an important role as the powerful oxidizing agent in AOPs and beneficial ROSs, RNSs, and RONSs productions, which influence the transformation of organic and polysaccharide structures [7], [10], [11], [12], [13], [65]. Regarding the OES observed at capturing time 1, it could be noticed that a broad spectrum has been observed, which is in contrast to the OESs observed at capturing times 2 and 3, where OESs perform a lower level of continuum radiation. This could be implied that the OES observed at capturing time 1 had been captured during the spark discharge mode, while others had been cap-

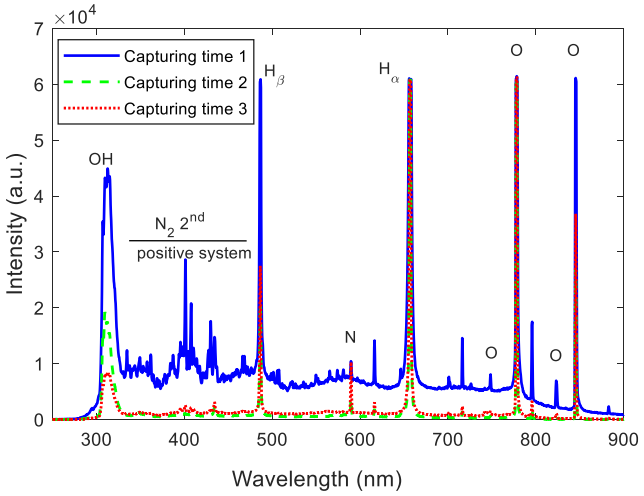

FIGURE 4. The optical emission spectra (OES) during the EBL process observed at 3 different capturing times.

tured during the corona streamer discharge mode. The broad spectrum of the OES observed at capturing time 1 has been influenced by black-body radiation due to the joule heating during the spark discharge. This phenomenon is consistent with the large leakage current causing an electro-thermal process resulting in high-temperature accumulation during the EBL process [52]. Moreover, the broad spectrum could also contribute from the molecular bands of molecules and molecular ions, such as the bands of 1^{st} positive, 1^{st} negative, and 2^{nd} positive N_2, which are usually found in the air discharge [66], [67], [68]. In contrast, the narrow OES bands have been contributed by the streamer, spark, and glow discharge of neutral atoms and atomic ion emission [49], [50], [51], [52], [69].

D. CHARACTERISTICS OF TREATED INULIN SOLUTION, ANTIOXIDANT ACTIVITY, AND PROBIOTIC ACTIVITY OF INULIN AFTER EBL PROCESS

The physical-chemical properties, including pH, temperature, H_2O_2, EC, and antioxidant activity (DPPH) of inulin solution, have been investigated before (0 min) and after the 20 min EBL process, as shown in Fig. 5. The variation tendency of solution temperature, EC, and antioxidant activity increases when the input voltage (output voltage) increases while the pH shows an opposite trend. However, the variation of these parameters is consistent [32], [36], [70], [71], [72], [73]. The chemical reactions between the air plasma and the treated inulin solution have caused the solution pH to fall. Typically, pH is measured as the negative logarithm of the concentration of hydrogen ions (H^+) in a solution. Various compounds, including hydrogen peroxide (H_2O_2), nitric acid (HNO_3), peroxynitrous acid (ONOOH), and others, were generated during and after the EBL process and contributed to the decrease in pH [32], [36], [72], [73], [74], [75], [76].

The EC of inulin solution has greatly risen due to numerous active ions generated during the EBL process [32], [36], [70], [71], [72]. The conductivity levels of the inulin solution generated at the input voltages of 110, 120, and 150 V_{rms} are higher than that of the control group, around 12, 23, and 29 times, respectively. The solution temperature after 20 min treatment slightly increased (owing to the cooling system) in the control group as in the same trend as EC. As input voltage increased, the solution pH values after 20 min treatment have dropped from 5.83±0.09 to 3.52±0.08, 3.27±0.07, and 2.86±0.10, respectively.Regarding the H_2O_2 strip test, it could be confirmed that the existence of H_2O_2 in all cases could be around or more than 25 mg L^{-1}.

The results, Fig. 5e) showed that the highest antioxidant activity of inulin came from the highest generating voltage (150 V_{rms} input) and longest treatment time (20 min). DPPH scavenging activity of 182.39±4.32 μg TE mL^{-1} was significantly improved by 311% compared with the control (untreated inulin) at 0 min (44.29±6.94 μg TE mL^{-1}). The increase in DPPH scavenging activity was increased with increasing voltage and treatment time. This implied that the structure of control inulin has been changed in some ways during plasma treatment and hence the increased antioxidant activity. Therefore, inulin at 150 V_{rms} input and 20 min treatment time was chosen for the prebiotic activity test. The results (Fig. 6) confirmed that the plasma treatment on inulin enhanced the prebiotic activity of inulin on *Lactococcus lactis* subsp. *lactis* TBRC 375. The growth of bacteria at 72 h from treated inulin ($OD_{600nm} = 0.54$) was higher than that of control inulin ($OD_{600nm} = 0.40$) by 35%. The bacterial growth without inulin as a prebiotic was significantly lower ($OD_{600nm} = 0.16$). At this plasma treatment condition, the antioxidant activity and the prebiotic activity of inulin were significantly improved by 311%, and 35%, respectively.

E. MORPHOLOGY OF INULIN STRUCTURE AFTER EBL PROCESS

The structural analysis of the inulin structure before and after the EBL process was investigated by SEM, as shown in Fig. 7. The morphology of the inulin structure before the EBL process in Fig. 7a) is similar to a micro spherical shape with a smooth surface having a diameter ranging from 20-100 μm [22]. It could be clearly seen that the inulin structures underwent complete fragmentation, segregation into distinct particles, and the interior portion experienced disruption, as shown in Fig. 7b), and hence possibly yielding lower molecular weight molecules. Regarding the SEM images, it could be confirmed that the EBL process could be a potential tool for biological transformation and/or modification of inulin by improving the accessibility of reactants, such as hydroxyl radicals generated during EBL process.

F. INFLUENCE OF THE EBL PROCESS ON INULIN STRUCTURAL TRANSFORMATIONS

In contrast to the electrical gas breakdown, the electrical discharges in liquid have a rather complicated breakdown mechanism. The breakdown mechanism in liquids is a more complicated process than that in solids or gases. This is due

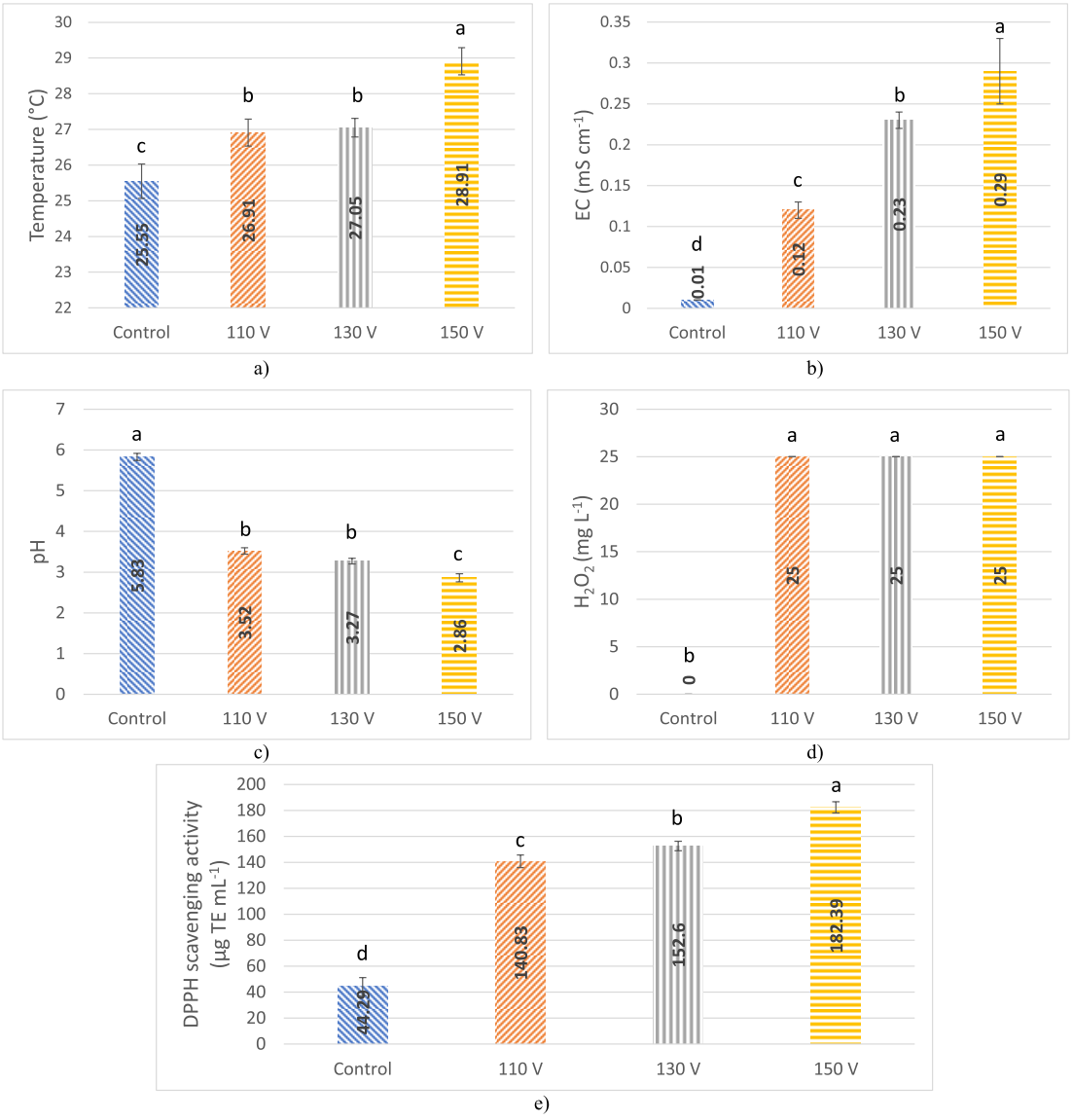

FIGURE 5. Inulin solution characteristics and its antioxidant activity at different input voltages, a) Temperature, b) EC, c) pH, d) H_2O_2, and e) DPPH scavenging activity. Superscripts on the bars indicate statistical significance at $p < 0.05$ using Duncan's multiple range test.

to the fact that liquids are denser than gases and lack the long-range order seen in solids. Moreover, the breakdown process is significantly influenced by electrode geometry, the characteristics of the supplied voltage, and the purity of the liquid, including dissolved gases, which can form microbubbles within the liquid [31], [32], [33], [34], [35]. However, the liquid-breakdown mechanism could be explained by the fundamentals of direct discharges in liquids owing to direct impact ionization and gas bubble theory. Generally, direct discharges in liquids are characterized by direct impact ionization, which necessitates the use of very short pulsed high voltage. Specifically, an electric field strength of at least 220 MV cm^{-1} with a rise time of a few picoseconds is required to facilitate this process. Therefore, this mechanism might not be applicable to the EBL process in this work.

The liquid breakdown mechanism of the EBL process can be explained using the gas bubble theory and in-bubble contacted discharge. Regarding the experimental results in section III-A, the EBL mechanism has been observed to function as follows: the corona streamer discharge generates a pre-breakdown phase by producing micro gas bubbles through joule heating at highly-stressed electrode tips in the liquid. Subsequently, over time, a streamer evolves and becomes a plasma column, which in turn triggers a spark streamer discharge upon the arrival of an air bubble in close proximity to it. This discharge expands owing to the non-uniform electric field distribution inside and outside the bubble. Ultimately, the breakdown is terminated as the air bubble deforms and passes through the electrode gap, thereby restarting the new cycle [31], [37], [38],

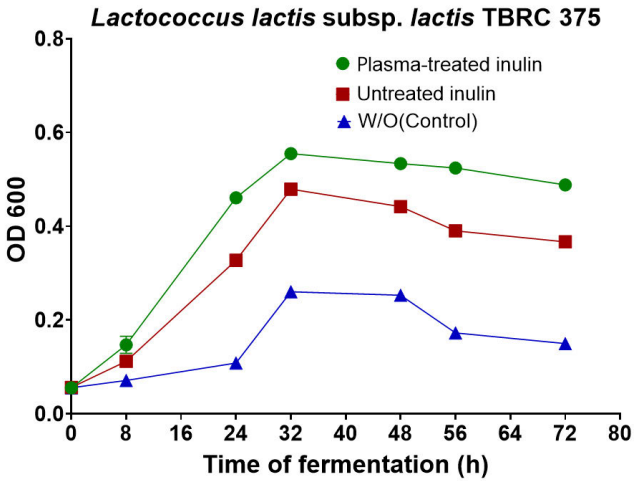

FIGURE 6. ***Lactococcus lactis*** **subsp.** ***lactis*** **TBRC 375 growth during 72 h fermentation with plasma-treated inulin, untreated inulin and without (w/o) inulin (negative control).**

[39], [40], [41], [42]. During each cycle, various species have been generated. Regarding the optical emission spectra in Fig. 4, there are various prominent peaks, such as H, O, OH·, N, NO, and molecular nitrogen bands. These species with energetic electrons and photons are the primary sources for other consequent reactions that resulted in other short-lived and long-lived species, such as O_2^-, $^1O_2$, O_2^{*-}, O_3, H_2O_2, NO_2^-, NO_3^-, including H_2O_2, HNO_3, and ONOOH. The chemical reactions during and after the EBL process could happen both in the gas phase, the gas-liquid interphase, and also the liquid phase. The most important primary substances, which are essential for biological applications, are O_2, H_2, N_2, and all forms of H_2O (vapor, droplet, gas, or liquid). A comprehensive description of potential chemical reactions during the EBL process can be found in [14], [36], [75], [76].

Even though, at present, the detailed mechanism of plasma-induced inulin structural modification has been the focus of our investigation, a brief explanation of the impact of the EBL process on the structural alteration of inulin could be possibly discussed. Regarding the studied parameters and evidence from the experiments and related research, the main reason for organic (inulin) structural transformations by the EBL process is from the physicochemical process [8], [13], [18], [77]. During the EBL process, several energetic, active, and reactive particles, species, radicals, and substances have been generated between the electrodes of the reactors. However, these particles have a different lifetime depending on their chemical species, and energy and momentum transfer [7], [8], [9], [32], [73], [74], [78]. Therefore, the AOPs are rather complicated, resulting from the chemical reactions between these particles. The structural modification has not just been active only at the electrode gap where air breakdown exists, but also in the treating solution owing to AOPs of the chemical reaction between the long-lived species and the organic structure dissolved in the solution.

In the liquid phase, the dissolved inulin structures have been continuously chemically reacted with the long- and short-lived reactive oxidant agents. It has been reported that the main reactive species playing an important role in the depolymerization process of polysaccharide structure are OH·, singlet O, O_3, nitric acid, and H_2O_2. Moreover, the excited species from the N_2 2^{nd} positive system detected in OES have contributed to surface modification in corporately with the reactive functional groups on the inulin (polysaccharide) surface [10], [11], [14], [20].

At the plasma-liquid interface region, though there has been only a short contacting time, inulin structures could possibly be directly in contact with air plasma; therefore, reactive species, UV radiation, a strong electromagnetic field, shock waves, fluid interface reactions, and other phenomena would interact with the inulin structure, directly resulting in plasma surface modification in both physical (etching and sputtering) and chemical interactions [8], [11], [20], [37], [42].

The hypothetical hydroxyl radical mechanism of inulin depolymerization by the EBL process is shown in Fig. 8. During the EBL process, hydroxyl radicals are produced from advanced oxidation process. These radicals have the ability to extract a hydrogen atom from the fructose unit located at the C-1 position of a β-(2, 1) glycosidic bond with the subsequent generation of a water molecule. Afterwards, the carbon radical was generated and underwent an oxidation reaction with oxygen within the system, resulting in the formation of a superoxide anion. As a result, the β-(2, 1) glycosidic bond of inulin underwent scission. Subsequently, the formation of the carbonyl group occurred, followed by the reaction of the C-2 radical with a hydroxyl radical, resulting in the production of oligomers with reducing ends of fructose units [14], [19], [21]. The hydroxyl radical-induced depolymerization of inulin has the potential to produce multiple oligomers [14], [65], which possess an increased number of reducing ends that can serve as effective reducing agents in reactions with oxidants. In addition, other radicals and phenomenon happening during the EBL process might possibly also contribute to this depolymerization of inulin [8], [11], [20], [37], [42]. As a result, the present study observed an increase in the antioxidant activity of plasma-treated inulin, as determined by the DPPH radical scavenging method, when compared to the control group consisting of untreated inulin. Likewise, the prebiotic effects of the smaller molecules of inulin oligomers were shown to be stronger compared to the untreated inulin control. This difference in effect may be attributed to the higher accessibility to beneficial bacteria, hence enhancing bacterial growth.

According to the experimental findings, it is possible to confirm that the electrical breakdown in the liquid (EBL) process significantly enhanced the antioxidant and prebiotic properties of the treated inulin solution, and also changed its morphology. However, the joule heating and the leakage current owing to the long-duty cycle of the high voltage applied

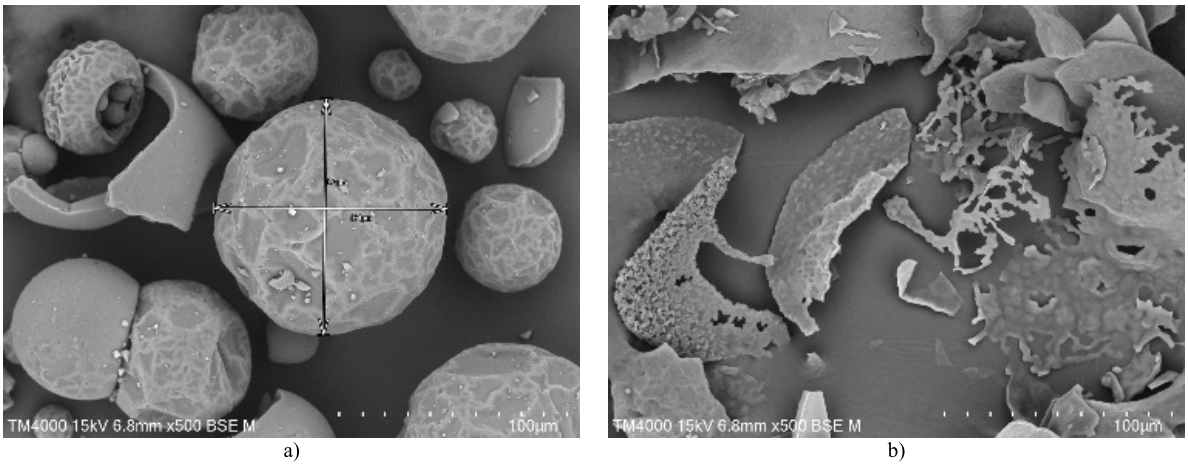

FIGURE 7. Example SEM images of inulin structures a) before and b) after 20 min EBL process.

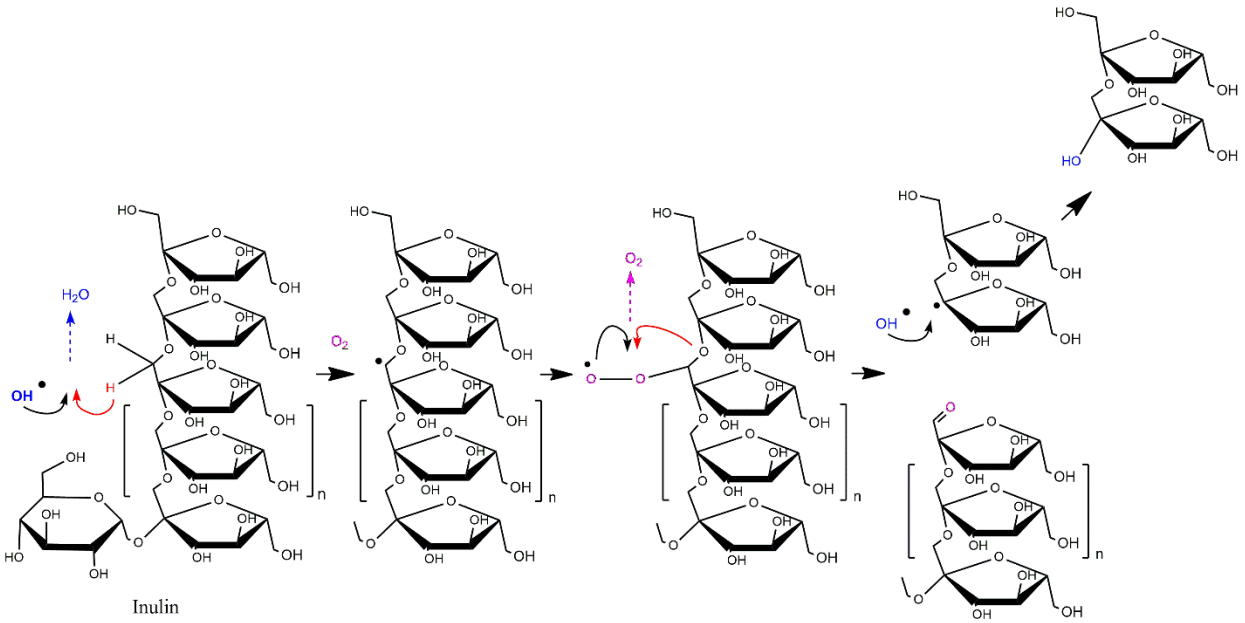

FIGURE 8. Hypothetical hydroxyl radical mechanism of inulin depolymerization by EBL process.

for the EBL generation, in the system are the issues that required to be improved. Nonetheless, the proposed method could possibly serve as an economically and promisingly green method for biotransformation, which is beneficial for bioactive functions and intrinsic viscosity enhancement [7], [10], [11], [12], [13], [14], [65].

IV. CONCLUSION

The electrical breakdown in the liquid (EBL) process has potential for inulin structural transformations and bioactivity enhancement. It has been found that the higher the voltage supplied for the EBL process within the critical optimal time, the better the outcome in terms of bioactivity. However, due to the long duty cycle of the supplied high voltage, the joule heating, and the leakage current could result in the accumulating heat in the treating liquid, and reduction of discharge voltage, which needs to be improved. The further study of this work is to determine the precise mechanism of plasma-induced inulin structural change, which is currently in progress. However, the suggested approach might be used as a promising, economically viable, and environmentally friendly strategy for biotransformation, which is advantageous for the enhancement of the inherent viscosity and bioactive activities of the other forms of polysaccharides from agricultural sources.

ACKNOWLEDGMENT

The authors would like to thank Srinakharinwirot University (SWU), Faculty of Engineering SWU, and Thailand

Institute of Nuclear Technology (TINT) for the support, and also would like to thank the advice and guidance from Associate Professor Dr. Weerasak Samee and Dr. Wasin Nupangtha regarding chemical reactions and optical emission spectroscopy analysis.

REFERENCES

[1] S. A. Razack, V. Velayutham, and V. Thangavelu, "Medium optimization for the production of exopolysaccharide by Bacillus subtilis using synthetic sources and agro wastes," *Turkish J. Biol.*, vol. 37, pp. 280–288, Jan. 2013, doi: 10.3906/biy-1206-50.

[2] F. Küçükaşik, "Molasses as fermentation substrate for Levan production by *Halomonas* sp.," *Appl. Microbiol. Biotechnol.*, vol. 89, no. 6, pp. 1729–1740, 2011, doi: 10.1007/s00253-010-3055-8.

[3] P. Seesuriyachan, A. Kuntiya, P. Hanmoungjai, and C. Techapun, "Exopolysaccharide production by lactobacillus confusus TISTR 1498 using coconut water as an alternative carbon source: The effect of peptone, yeast extract and beef extract," *Songklanakarin J. Sci. Technol.*, vol. 33, no. 4, pp. 379–387, 2011.

[4] A. U. Illippangama, D. D. Jayasena, C. Jo, and D. C. Mudannayake, "Inulin as a functional ingredient and their applications in meat products," *Carbohydrate Polym.*, vol. 275, Jan. 2022, Art. no. 118706, doi: 10.1016/j.carbpol.2021.118706.

[5] F. M. Clark, "The electrical breakdown of liquid dielectrics," *J. Franklin Inst.*, vol. 216, no. 4, pp. 429–458, Oct. 1933, doi: 10.1016/S0016-0032(33)90914-X.

[6] P. Wedin, "Electrical breakdown in dielectric liquids—A short overview," *IEEE Elect. Insul. Mag.*, vol. 30, no. 6, pp. 20–25, Nov. 2014, doi: 10.1109/MEI.2014.6943430.

[7] Y. Deng and R. Zhao, "Advanced oxidation processes (AOPs) in wastewater treatment," *Current Pollut. Rep.*, vol. 1, no. 3, pp. 167–176, Sep. 2015, doi: 10.1007/s40726-015-0015-z.

[8] N. Saito, M. A. Bratescu, and K. Hashimi, "Solution plasma: A new reaction field for nanomaterials synthesis," *Japanese J. Appl. Phys.*, vol. 57, no. 1, Jan. 2018, Art. no. 0102A4, doi: 10.7567/JJAP.57.0102A4.

[9] S. Horikoshi and N. Serpone, "In-liquid plasma: A novel tool in the fabrication of nanomaterials and in the treatment of wastewaters," *RSC Adv.*, vol. 7, no. 75, pp. 47196–47218, 2017, doi: 10.1039/c7ra09600c.

[10] R. Nastase, J. Tatibouët, and E. Fourré, "Depolymerization of inulin in the highly reactive gas phase of a non thermal plasma at atmospheric pressure," *Plasma Processes Polym.*, vol. 15, no. 10, Oct. 2018, Art. no. 1800067, doi: 10.1002/ppap.201800067.

[11] R. Nastase, E. Fourré, M. Fanuel, X. Falourd, and I. Capron, "Non thermal plasma in liquid media: Effect on inulin depolymerization and functionalization," *Carbohydrate Polym.*, vol. 231, Mar. 2020, Art. no. 115704, doi: 10.1016/j.carbpol.2019.115704.

[12] T. Tantiplapol, Y. Singsawat, N. Narongsil, S. Damrongsakkul, N. Saito, and I. Prasertsung, "Influences of solution plasma conditions on degradation rate and properties of chitosan," *Innov. Food Sci. Emerg. Technol.*, vol. 32, pp. 116–120, Dec. 2015, doi: 10.1016/j.ifset.2015.09.014.

[13] F. Ma, J. Wu, P. Li, D. Tao, H. Zhao, B. Zhang, and B. Li, "Effect of solution plasma process with hydrogen peroxide on the degradation of water-soluble polysaccharide from auricularia auricula. II: Solution conformation and antioxidant activities in vitro," *Carbohydrate Polym.*, vol. 198, pp. 575–580, Oct. 2018, doi: 10.1016/j.carbpol.2018.06.113.

[14] S. Sangwanna, W. Seelarat, T. Panklai, N. Chaosuan, A. Subcharoen, N. Subcharoen, N. Chanchula, T. Inyod, T. Toemarrom, A. Bootchanont, C. Wattanawikkam, S. Pavasupree, D. Boonyawan, and P. Porjai, "Air atmospheric pressure plasma jet to improve fruiting body production and enhance bioactive phytochemicals from mutant cordyceps militaris (white cordyceps militaris)," *Food Bioprocess Technol.*, vol. 16, no. 9, pp. 1976–1991, Sep. 2023, doi: 10.1007/s11947-023-03028-x.

[15] M. A. Habib, S. Hosseini, T. Sakugawa, and H. Akiyama, "Treatment of wastewater by underwater discharge in gas bubbling water," *Int. J. Renew. Energy Environ. Eng.*, vol. 3, no. 3, pp. 189–194, 2015.

[16] K. Matra and S. Tawkaew, "Decolorization of methylene blue in an Ar non-thermal plasma reactor," *J. Eng. Sci. Technol. Rev.*, vol. 13, no. 1, pp. 114–119, Feb. 2020, doi: 10.25103/jestr.131.15.

[17] S. Theepharaksapan and K. Matra, "Atmospheric argon plasma jet for post-treatment of biotreated landfill leachate," in *Proc. Int. Electr. Eng. Congr. (iEECON)*, Mar. 2018, pp. 1–4, doi: 10.1109/IEECON.2018.8712320.

[18] F. Ma, P. Li, B. Zhang, X. Zhao, Q. Fu, Z. Wang, and C. Gu, "Effect of solution plasma process with bubbling gas on physicochemical properties of chitosan," *Int. J. Biol. Macromolecules*, vol. 98, pp. 201–207, May 2017, doi: 10.1016/j.ijbiomac.2017.01.049.

[19] I. Prasertsung, P. Chutinate, A. Watthanaphanit, N. Saito, and S. Damrongsakkul, "Conversion of cellulose into reducing sugar by solution plasma process (SPP)," *Carbohydrate Polym.*, vol. 172, pp. 230–236, Sep. 2017, doi: 10.1016/j.carbpol.2017.05.025.

[20] C. M. Laureano-Anzaldo, M. E. González-López, A. A. Pérez-Fonseca, L. E. Cruz-Barba, and J. R. Robledo-Ortíz, "Plasma-enhanced modification of polysaccharides for wastewater treatment: A review," *Carbohydrate Polym.*, vol. 252, Jan. 2021, Art. no. 117195, doi: 10.1016/j.carbpol.2020.117195.

[21] I. Prasertsung, K. Aroonraj, K. Kamwilaisak, N. Saito, and S. Damrongsakkul, "Production of reducing sugar from cassava starch waste (CSW) using solution plasma process (SPP)," *Carbohydrate Polym.*, vol. 205, pp. 472–479, Feb. 2019, doi: 10.1016/j.carbpol.2018.10.090.

[22] H. Qiao, T. Zhao, J. Yin, Y. Zhang, H. Ran, S. Chen, Z. Wu, R. Zhang, X. Wang, L. Gan, and J. Wang, "Structural characteristics of inulin and microcrystalline cellulose and their effect on ameliorating colitis and altering colonic microbiota in dextran sodium sulfate-induced colitic mice," *ACS Omega*, vol. 7, no. 13, pp. 10921–10932, Apr. 2022, doi: 10.1021/acsomega.1c06552.

[23] T. Shao, Q. Yu, T. Zhu, A. Liu, X. Gao, X. Long, and Z. Liu, "Inulin from Jerusalem artichoke tubers alleviates hyperglycaemia in high-fat-diet-induced diabetes mice through the intestinal microflora improvement," *Brit. J. Nutrition*, vol. 123, no. 3, pp. 308–318, Feb. 2020, doi: 10.1017/S0007114519002332.

[24] B. R. Shah, B. Li, H. Al Sabbah, W. Xu, and J. Mráz, "Effects of prebiotic dietary fibers and probiotics on human health: With special focus on recent advancement in their encapsulated formulations," *Trends Food Sci. Technol.*, vol. 102, pp. 178–192, Aug. 2020, doi: 10.1016/j.tifs.2020.06.010.

[25] A. C. Apolinário, B. P. G. de Lima Damasceno, N. E. de Macêdo Beltrão, A. Pessoa, A. Converti, and J. A. da Silva, "Inulin-type fructans: A review on different aspects of biochemical and pharmaceutical technology," *Carbohydrate Polym.*, vol. 101, pp. 368–378, Jan. 2014, doi: 10.1016/j.carbpol.2013.09.081.

[26] C. Dechthummarong and K. Matra, "An investigation of plasma activated water generated by 50 Hz half wave AC high voltage," in *Proc. Int. Electr. Eng. Congr. (iEECON)*, Mar. 2018, pp. 1–4, doi: 10.1109/IEECON.2018.8712312.

[27] A. Khlyustova, N. Sirotkin, I. Naumova, A. Tarasov, and V. Titov, "Solution plasma processing as an environmentally friendly method for low-molecular chitosan production," *Plasma Chem. Plasma Process.*, vol. 42, no. 3, pp. 587–603, May 2022, doi: 10.1007/s11090-022-10237-3.

[28] K. Matra, W. Saengha, T. Karirat, K. Nakhowong, P. Pattanu, P. Kitkayun, T. Bubpamala, B. Buranrat, T. Katisart, and V. Luang-In, "Antioxidant activity of mustard green and Thai rat-tailed radish grown from cold plasma treated seeds and their anticancer efficacy against A549 lung cancer cells," *Notulae Botanicae Horti Agrobotanici Cluj-Napoca*, vol. 50, no. 2, p. 12751, May 2022, doi: 10.15835/nbha50212751.

[29] D. Z. Pai, D. A. Lacoste, and C. O. Laux, "Transitions between corona, glow, and spark regimes of nanosecond repetitively pulsed discharges in air at atmospheric pressure," *J. Appl. Phys.*, vol. 107, no. 9, May 2010, Art. no. 093303, doi: 10.1063/1.3309758.

[30] E. Kuffel, W. S. Zaengl, and J. Kuffel, "Electrostatic fields and field stress control," in *High Voltage Engineering Fundamentals*. Amsterdam, The Netherlands: Elsevier, 2000, pp. 201–280.

[31] V. M. Atrazhev, V. S. Vorob'ev, I. V. Timoshkin, M. J. Given, and S. J. MacGregor, "Mechanisms of impulse breakdown in liquid: The role of Joule heating and formation of gas cavities," *IEEE Trans. Plasma Sci.*, vol. 38, no. 10, pp. 2644–2651, Oct. 2010, doi: 10.1109/TPS.2010.2046337.

[32] P. J. Bruggeman et al., "Plasma–liquid interactions: A review and roadmap," *Plasma Sources Sci. Technol.*, vol. 25, no. 5, Sep. 2016, Art. no. 053002, doi: 10.1088/0963-0252/25/5/053002.

[33] A. Sun, C. Huo, and J. Zhuang, "Formation mechanism of streamer discharges in liquids: A review," *High Voltage*, vol. 1, no. 2, pp. 74–80, Jul. 2016, doi: 10.1049/hve.2016.0016.

[34] R. P. Joshi and S. M. Thagard, "Streamer-like electrical discharges in water: Part II. Environmental applications," *Plasma Chem. Plasma Process.*, vol. 33, no. 1, pp. 17–49, Feb. 2013, doi: 10.1007/s11090-013-9436-x.

[35] R. P. Joshi and S. M. Thagard, "Streamer-like electrical discharges in water: Part I. Fundamental mechanisms," *Plasma Chem. Plasma Process.*, vol. 33, no. 1, pp. 1–15, Feb. 2013, doi: 10.1007/s11090-012-9425-5.
[36] R. Thirumdas, A. Kothakota, U. Annapure, K. Siliveru, R. Blundell, R. Gatt, and V. P. Valdramidis, "Plasma activated water (PAW): Chemistry, physico-chemical properties, applications in food and agriculture," *Trends Food Sci. Technol.*, vol. 77, pp. 21–31, Jul. 2018, doi: 10.1016/j.tifs.2018.05.007.
[37] S. Liu, Y. Liu, X. Li, Z. Li, G. Zhou, Q. Zhang, H. Li, and F. Lin, "Effect of electrical breakdown discharge modes on shock wave intensity in water," in *Proc. IEEE 19th Int. Conf. Dielectr. Liquids (ICDL)*, Jun. 2017, pp. 1–5, doi: 10.1109/ICDL.2017.8124690.
[38] S. M. Korobeynikov and Y. N. Sinikh, "Bubbles and breakdown of liquid dielectrics," in *Proc. Conf. Rec. IEEE Int. Symp. Electr. Insul.*, Feb. 1998, pp. 603–606, doi: 10.1109/ELINSL.1998.694865.
[39] R. Zhang, Q. Zhang, C. Guo, X. He, Z. Wu, and T. Wen, "Bubbles in transformer oil: Dynamic behavior, internal discharge, and triggered liquid breakdown," *IEEE Trans. Dielectr. Electr. Insul.*, vol. 29, no. 1, pp. 86–94, Feb. 2022, doi: 10.1109/TDEI.2022.3148484.
[40] Z. Wang, W. Yan, K. Yang, L. Sun, Z. Liu, Y. Geng, and J. Wang, "The influence of liquid viscosities on bubble breakdown," in *Proc. 4th Int. Conf. Electr. Power Equip. Switching Technol. (ICEPE-ST)*, Oct. 2017, pp. 624–627, doi: 10.1109/ICEPE-ST.2017.8188922.
[41] N. Y. Babaeva, D. V. Tereshonok, and G. V. Naidis, "Initiation of breakdown in bubbles immersed in liquids: Pre-existed charges versus bubble size," *J. Phys. D, Appl. Phys.*, vol. 48, no. 35, Sep. 2015, Art. no. 355201, doi: 10.1088/0022-3727/48/35/355201.
[42] K. T. Sunao Katsuki, "Shock wave due to pulsed streamer discharges in water," in *Proc. Conf. Rec. 26th Int. Power Modulator Symp., High-Voltage Workshop*, 2004, pp. 607–610, doi: 10.1109/MODSYM.2004.1433650.
[43] K. Matra, "DC non-thermal atmospheric-pressure plasma jet generated using a syringe needle electrode," *Jpn. J. Appl. Phys.*, vol. 55, no. 7S2, Jul. 2016, Art. no. 07LB02, doi: 10.7567/JJAP.55.07LB02.
[44] K. Matra, "Atmospheric non-thermal argon–oxygen plasma for sunflower seedling growth improvement," *Jpn. J. Appl. Phys.*, vol. 57, no. 1S, Jan. 2018, Art. no. 01AG03.
[45] G. B. Sretenović, M. Saleem, O. Biondo, G. Tomei, E. Marotta, and C. Paradisi, "Spectroscopic study of self-pulsing discharge with liquid electrode," *J. Appl. Phys.*, vol. 129, no. 18, May 2021, Art. no. 183308, doi: 10.1063/5.0044331.
[46] J. Pawłat, P. Terebun, M. Kwiatkowski, B. Tarabová, Z. Kovalová, K. Kučerová, Z. Machala, M. Janda, and K. Hensel, "Evaluation of oxidative species in gaseous and liquid phase generated by mini-gliding arc discharge," *Plasma Chem. Plasma Process.*, vol. 39, no. 3, pp. 627–642, May 2019, doi: 10.1007/s11090-019-09974-9.
[47] S. Nijdam, J. Teunissen, and U. Ebert, "The physics of streamer discharge phenomena," *Plasma Sources Sci. Technol.*, vol. 29, no. 10, Nov. 2020, Art. no. 103001, doi: 10.1088/1361-6595/abaa05.
[48] L. Gao, "Measurement of the positive streamer charge," in *Proc. 11th Int. Symp. High-Voltage Eng. (ISH)*, 1999, p. V3-35, doi: 10.1049/cp:19990693.
[49] B. Sun, M. Sato, A. Harano, and J. Clements, "Non-uniform pulse discharge-induced radical production in distilled water," *J. Electrostat.*, vol. 43, no. 2, pp. 115–126, Apr. 1998, doi: 10.1016/S0304-3886(97)00166-6.
[50] X. Lu, Y. Pan, K. Liu, M. Liu, and H. Zhang, "Spark model of pulsed discharge in water," *J. Appl. Phys.*, vol. 91, no. 1, pp. 24–31, Jan. 2002, doi: 10.1063/1.1420765.
[51] P. Vanraes, A. Nikiforov, and C. Leys, "Electrical and spectroscopic characterization of underwater plasma discharge inside rising gas bubbles," *J. Phys. D, Appl. Phys.*, vol. 45, no. 24, Jun. 2012, Art. no. 245206, doi: 10.1088/0022-3727/45/24/245206.
[52] S.-W. Liu, Y. Liu, Y.-J. Ren, F.-C. Lin, and Y. Liu, "Characteristic analysis of plasma channel and shock wave in electrohydraulic pulsed discharge," *Phys. Plasmas*, vol. 26, no. 9, Sep. 2019, Art. no. 093509, doi: 10.1063/1.5092362.
[53] J. Kornev, N. Yavorovsky, S. Preis, M. Khaskelberg, U. Isaev, and B.-N. Chen, "Generation of active oxidant species by pulsed dielectric barrier discharge in water-air mixtures," *Ozone, Sci. Eng.*, vol. 28, no. 4, pp. 207–215, Aug. 2006, doi: 10.1080/01919510600704957.
[54] K. Matra, P. Buppan, and B. Techaumnat, "Analytical and experimental studies on the application of a series of treatment chambers for *Escherichia coli* inactivation by pulsed electric fields," *Appl. Sci.*, vol. 10, no. 12, p. 4071, Jun. 2020, doi: 10.3390/APP10124071.
[55] P. Bruggeman, C. Leys, and J. Vierendeels, "Experimental investigation of DC electrical breakdown of long vapour bubbles in capillaries," *J. Phys. D, Appl. Phys.*, vol. 40, no. 7, pp. 1937–1943, Apr. 2007, doi: 10.1088/0022-3727/40/7/016.
[56] S. J. Zheng, Y. C. Zhang, B. Ke, F. Ding, Z. L. Tang, K. Yang, and X. D. Zhu, "Dynamic characteristics of gas-water interfacial plasma under water," *Phys. Plasmas*, vol. 19, no. 6, Jun. 2012, Art. no. 063507, doi: 10.1063/1.4731699.
[57] Z. Chen, L. Lin, X. Cheng, E. Gjika, and M. Keidar, "Effects of cold atmospheric plasma generated in deionized water in cell cancer therapy," *Plasma Processes Polym.*, vol. 13, no. 12, pp. 1151–1156, Dec. 2016, doi: 10.1002/ppap.201600086.
[58] I.-E. Vlad and S. D. Anghel, "Time stability of water activated by different on-liquid atmospheric pressure plasmas," *J. Electrostatics*, vol. 87, pp. 284–292, Jun. 2017, doi: 10.1016/j.elstat.2017.06.002.
[59] X. Cheng, J. Sherman, W. Murphy, E. Ratovitski, J. Canady, and M. Keidar, "The effect of tuning cold plasma composition on glioblastoma cell viability," *PLoS ONE*, vol. 9, no. 5, pp. 1–9, 2014, doi: 10.1371/journal.pone.0098652.
[60] J. L. Walsh and M. G. Kong, "Contrasting characteristics of linear-field and cross-field atmospheric plasma jets," *Appl. Phys. Lett.*, vol. 93, no. 11, Sep. 2008, Art. no. 111501, doi: 10.1063/1.2982497.
[61] Y. Li, J. H. Kim, E. H. Choi, and I. Han, "Promotion of osteogenic differentiation by non-thermal biocompatible plasma treated chitosan scaffold," *Sci. Rep.*, vol. 9, no. 1, pp. 1–10, Mar. 2019, doi: 10.1038/s41598-019-40371-6.
[62] P. Thana, A. Wijaikhum, P. Poramapijitwat, C. Kuensaen, J. Meerak, A. Ngamjarurojana, S. Sarapirom, and D. Boonyawan, "A compact pulse-modulation cold air plasma jet for the inactivation of chronic wound bacteria: Development and characterization," *Heliyon*, vol. 5, no. 9, Sep. 2019, Art. no. e02455, doi: 10.1016/j.heliyon.2019.e02455.
[63] N. N. Misra, K. M. Keener, P. Bourke, and P. J. Cullen, "Generation of in-package cold plasma and efficacy assessment using methylene blue," *Plasma Chem. Plasma Process.*, vol. 35, no. 6, pp. 1043–1056, Nov. 2015, doi: 10.1007/s11090-015-9638-5.
[64] Y. H. Kim, Y. J. Hong, K. Y. Baik, G. C. Kwon, J. J. Choi, G. S. Cho, H. S. Uhm, D. Y. Kim, and E. H. Choi, "Measurement of reactive hydroxyl radical species inside the biosolutions during non-thermal atmospheric pressure plasma jet bombardment onto the solution," *Plasma Chem. Plasma Process.*, vol. 34, no. 3, pp. 457–472, May 2014, doi: 10.1007/s11090-014-9538-0.
[65] H. Barreteau, C. Delattre, and P. Michaud, "Production of oligosaccharides as promising new food additive generation," *Food Technol. Biotechnol.*, vol. 44, no. 3, pp. 323–333, Nov. 2005.
[66] D. M. Devia, L. V. Rodriguez-Restrepo, and E. Restrepo-Parra, "Methods employed in optical emission spectroscopy analysis: A review," *Ingeniería y Ciencia*, vol. 11, no. 21, pp. 239–267, Feb. 2015, doi: 10.17230/ingciencia.11.21.12.
[67] Z. Ahmad, G. B. Cross, M. Vernon, D. Gebregiorgis, D. Deocampo, and A. Kozhanov, "Influence of plasma-activated nitrogen species on PA-MOCVD of InN," *Appl. Phys. Lett.*, vol. 115, no. 22, Nov. 2019, Art. no. 223101, doi: 10.1063/1.5126625.
[68] P. Attri and E. H. Choi, "Influence of reactive oxygen species on the enzyme stability and activity in the presence of ionic liquids," *PLoS ONE*, vol. 8, no. 9, Sep. 2013, Art. no. e75096, doi: 10.1371/journal.pone.0075096.
[69] S. Wang, F. Liu, D.-Z. Yang, W. Wang, and Z. Fang, "Characteristic study of a transient spark driven by a nanosecond pulse power in atmospheric nitrogen using a water cathode," *J. Appl. Phys.*, vol. 125, no. 4, Jan. 2019, Art. no. 043304, doi: 10.1063/1.5050259.
[70] J. S. Clements, M. Sato, and R. H. Davis, "Preliminary investigation of prebreakdown phenomena and chemical reactions using a pulsed high-voltage discharge in water," *IEEE Trans. Ind. Appl.*, vol. IA-23, no. 2, pp. 224–235, Mar. 1987, doi: 10.1109/TIA.1987.4504897.
[71] B. Sun, M. Sato, and J. Sid Clements, "Optical study of active species produced by a pulsed streamer corona discharge in water," *J. Electrostatics*, vol. 39, no. 3, pp. 189–202, Jul. 1997, doi: 10.1016/S0304-3886(97)00002-8.
[72] J. Julák, A. Hujacová, V. Scholtz, J. Khun, and K. Holada, "Contribution to the chemistry of plasma-activated water," *Plasma Phys. Rep.*, vol. 44, no. 1, pp. 125–136, Jan. 2018, doi: 10.1134/S1063780X18010075.
[73] K. Matra, Y. Tanakaran, V. Luang-In, and S. Theepharaksapan, "Enhancement of lettuce growth by PAW spray gliding arc plasma generator," *IEEE Trans. Plasma Sci.*, vol. 50, no. 6, pp. 1430–1439, Jun. 2022, doi: 10.1109/TPS.2021.3105733.

[74] S. Theepharaksapan, Y. Lerkmahalikhit, P. Suwannapech, P. Boonnong, M. Limawatchanakarn, and K. Matra, "Impact of multi-air plasma jets on nitrogen concentration variance in effluent of membrane bioreactor pilot-plant," *Eng. Appl. Sci. Res.*, vol. 48, no. 6, pp. 732–739, 2021, doi: 10.14456/easr.2021.75.
[75] N. K. Kaushik, B. Ghimire, Y. Li, M. Adhikari, M. Veerana, N. Kaushik, N. Jha, B. Adhikari, S.-J. Lee, K. Masur, T. von Woedtke, K.-D. Weltmann, and E. H. Choi, "Biological and medical applications of plasma-activated media, water and solutions," *Biol. Chem.*, vol. 400, no. 1, pp. 39–62, Dec. 2018, doi: 10.1515/hsz-2018-0226.
[76] B. R. Locke, P. Lukes, and J. Brisset, "Elementary chemical and physical phenomena in electrical discharge plasma in gas-liquid environments and in liquids," in *Plasma Chemistry and Catalysis in Gases and Liquids*. Hoboken, NJ, USA: Wiley, 2012, pp. 185–241.
[77] Z.-L. Chen, C. Wang, H. Ma, Y. Ma, and J.-K. Yan, "Physicochemical and functional characteristics of polysaccharides from okra extracted by using ultrasound at different frequencies," *Food Chem.*, vol. 361, Nov. 2021, Art. no. 130138, doi: 10.1016/j.foodchem.2021.130138.
[78] F. Judée, S. Simon, C. Bailly, and T. Dufour, "Plasma-activation of tap water using DBD for agronomy applications: Identification and quantification of long lifetime chemical species and production/consumption mechanisms," *Water Res.*, vol. 133, pp. 47–59, Apr. 2018, doi: 10.1016/j.watres.2017.12.035.

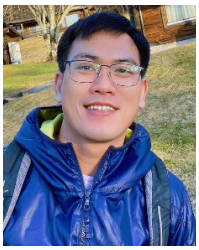

KHANIT MATRA received the B.Eng. degree (Hons.) and the M.Eng. degree in electrical engineering from Khon Kaen University, Thailand, in 2007 and 2009, respectively, and the Ph.D. degree in electronics and photonics systems engineering from the Kochi University of Technology, Japan, in 2013.

Currently, he is an Associate Professor with the Department of Electrical Engineering, Faculty of Engineering, Srinakharinwirot University, Thailand. His research interests include microplasma characteristics, high voltage engineering, atmospheric non-thermal plasma applications, and other emerging technologies.

WANATTAPONG ARYUWONG received the bachelor's degree in electrical engineering (power) from the Department of Electrical Engineering, Srinakharinwirot University, Nakhon Nayok, Thailand, in 2022. His research interest includes the potential of plasma-activated water as a liquid nitrogen fertilizer for micro-algae cultivation.

WICHAYADA MEETANG received the bachelor's degree in electrical engineering (power) from the Department of Electrical Engineering, Srinakharinwirot University, Nakhon Nayok, Thailand, in 2022. Her research interest includes applying electrical breakdown in liquid processes on biological structural transformations.

SUPARADA RUTHAIRAT received the bachelor's degree in electrical engineering (power) from the Department of Electrical Engineering, Srinakharinwirot University, Nakhon Nayok, Thailand, in 2022. Her research interest includes the application of electrical breakdown in liquid processes on biological structural transformations.

CHANCHAI DECHTHUMMARONG was born in Chiang Mai, Thailand, in 1969. He received the B.S. degree in electrical engineering from the Rajamangala Institute of Technology, Thailand, in 1992, the M.S. degree in electrical engineering from Chiang Mai University, Thailand, in 1996, and the Ph.D. degree in energy technology from the King Mongkut's University of Technology Thonburi, Bangkok, Thailand, in 2012.

He studied the design of high voltage generators and the testing of high voltage insulation, since 1992, during the master's and Ph.D. degrees. In 1998, he joined to Electrical Engineering Department, Faculty of Engineering, Rajamangala University of Technology Lanna (RMUTL), Chiang Mai, Thailand, as a Lecturer in the field of high voltage engineering. During working at RMUTL, he has been researching various high-voltage power supplies for generating cold atmospheric-pressure plasma in the gap. His current research interests include the development of high voltage power supply technologies for discharge plasma in contact not only with traditional solutions, but also in gas-liquid mixture solutions. The goal of his research is to improve agricultural productivity and quality and environmental applications using high-voltage stimulations, plasma-activated solutions, and ultrafine bubbles with better engineering system design processes of the best optimum performance.

WUTTHICHOK SANGWANG received the B.Eng. and M.Eng. degrees in electrical engineering from Srinakharinwirot University (SWU), Bangkok, Thailand, in 2017 and 2023, respectively. Currently, he is a Nuclear Engineer with the Thailand Institute of Nuclear Technology (Public Organization), Thailand. His research interests include non-thermal plasma, plasma-activated water, high-voltage power supply, the electric field of characteristics, nuclear fusion, cyclotron machines, and other electrical technologies.

VIJITRA LUANG-IN received the B.Sc. degree (Hons.) in biotechnology, the M.Res. degree in biochemical research, and the Ph.D. degree in biochemistry from Imperial College London, London, U.K., in 2008, 2009, and 2013, respectively. She is currently an Associate Professor with the Department of Biotechnology, Faculty of Technology, Mahasarakham University, Mahasarakham, Thailand. Her research interests include applied microbiology, cancer biology, phytochemicals, and the applications of plasma technology in life sciences.